REPORT DOCUMENTATION PAGE

Form Approved
OMB No. 0704-0188

1. REPORT DATE *(DD-MM-YYYY)*	**2. REPORT TYPE**	**3. DATES COVERED** *(From - To)*
24-03-2006	Technical Paper	

4. TITLE AND SUBTITLE

Behavior of a Rocket-Like Coaxial Injector in an Acoustic Field (POSTPRINT)

5a. CONTRACT NUMBER

5b. GRANT NUMBER

5c. PROGRAM ELEMENT NUMBER

6. AUTHOR(S)
D.W. Davis & B. Chehroudi (ERC, Inc.); D.G. Talley (AFRL/PRSA)

5d. PROJECT NUMBER
23080533

5e. TASK NUMBER

5f. WORK UNIT NUMBER

7. PERFORMING ORGANIZATION NAME(S) AND ADDRESS(ES)

Air Force Research Laboratory (AFMC)
AFRL/PRSA
10 E. Saturn Blvd.
Edwards AFB CA 93524-7680

8. PERFORMING ORGANIZATION REPORT NUMBER

AFRL-PR-ED-TP-2006-089

9. SPONSORING / MONITORING AGENCY NAME(S) AND ADDRESS(ES)

Air Force Research Laboratory (AFMC)
AFRL/PRS
5 Pollux Drive
Edwards AFB CA 93524-70448

10. SPONSOR/MONITOR'S ACRONYM(S)

11. SPONSOR/MONITOR'S NUMBER(S)
AFRL-PR-ED-TP-2006-089

12. DISTRIBUTION / AVAILABILITY STATEMENT

Approved for public release; distribution unlimited (AFRL-ERS-PAS-2006-072)

13. SUPPLEMENTARY NOTES
Presented at the Institute for Liquid Atomization and Spray Systems (ILASS) – Americas Meeting, Toronto, Canada, 23-26 May 2006.

14. ABSTRACT

A non-reacting-flow experimental investigation was undertaken to gain a better understanding of some of the underlying physics associated with the interaction of acoustic waves and a coaxial-jet injector similar to those used in cryogenic liquid rockets. Liquid nitrogen (the round inner jet) and gaseous nitrogen (the annular outer jet) were used under subcritical, near critical, and supercritical chamber pressures, with and without acoustic excitation. High-speed digital imaging provided information on the dynamic behavior of the jet under a variety of conditions. It is found that when the jet is at the pressure node, an externally-imposed acoustic field excites the dark-core of the jet to a wavy-shaped structure consistent with the field's characteristics. Mean and root mean square (RMS) values of the dark-core length fluctuations were measured from images. It is seen that as the outer-to-inner-jet velocity ratio increases, the RMS of the dark-core length fluctuations decreases both with and without the existence of the acoustic field. It is thought that a connection to the rocket instability may be established from these data through examination of the RMS values. It is possible that decreases in the fluctuation levels, shown to occur at higher velocity ratios, could weaken a key feedback mechanism for the self-excitation process that could be driving combustion instability in rocket engines. This could offer a possible explanation of the combustion stability improvements experienced in engines when a transition to higher values of the outer-to-inner-jet velocity ratio is made. Finally, after a careful review of relevant data taken here and those by others, there appears to be a good correlation between the dark-core length and the momentum flux ratio

15. SUBJECT TERMS

16. SECURITY CLASSIFICATION OF:			**17. LIMITATION OF ABSTRACT**	**18. NUMBER OF PAGES**	**19a. NAME OF RESPONSIBLE PERSON**
					Dr. Douglas G. Talley
a. REPORT	**b. ABSTRACT**	**c. THIS PAGE**	A	13	**19b. TELEPHONE NUMBER** *(include area code)*
Unclassified	**Unclassified**	**Unclassified**			N/A

Behavior of a Rocket-Like Coaxial Injector in an Acoustic Field

D. W. Davis* and B. Chehroudi
ERC, Inc., Edwards AFB, CA

D.G. Talley
Air Force Research Laboratory, Edwards AFB, CA

Abstract

A non-reacting-flow experimental investigation was undertaken to gain a better understanding of some of the underlying physics associated with the interaction of acoustic waves and a coaxial-jet injector similar to those used in cryogenic liquid rockets. Liquid nitrogen (the round inner jet) and gaseous nitrogen (the annular outer jet) were used under subcritical, near critical, and supercritical chamber pressures, with and without acoustic excitation. High-speed digital imaging provided information on the dynamic behavior of the jet under a variety of conditions. It is found that when the jet is at the pressure node, an externally-imposed acoustic field excites the dark-core of the jet to a wavy-shaped structure consistent with the field's characteristics. Mean and root mean square (RMS) values of the dark-core length fluctuations were measured from images. It is seen that as the outer-to-inner-jet velocity ratio increases, the RMS of the dark-core length fluctuations decreases both with and without the existence of the acoustic field. It is thought that a connection to the rocket instability may be established from these data through examination of the RMS values. It is possible that decreases in the fluctuation levels, shown to occur at higher velocity ratios, could weaken a key feedback mechanism for the self-excitation process that could be driving combustion instability in rocket engines. This could offer a possible explanation of the combustion stability improvements experienced in engines when a transition to higher values of the outer-to-inner-jet velocity ratio is made. Finally, after a careful review of relevant data taken here and those by others, there appears to be a good correlation between the dark-core length and the momentum flux ratio

Introduction

Combustion instabilities in liquid rocket engines (LREs) can reach amplitudes of 100% of chamber pressure and damage an engine in a fraction of a second [1,2]. The combustion instability mechanisms span from low-frequency mechanisms, which is a feed-system coupled instability, to high-frequency mechanisms, which depend on the acoustic modes of the chamber. Often LRE's operate at chamber pressures which exceed the critical pressure of the propellants. In such cases, while the pressure is supercritical, the initial temperature of the propellants is often subcritical, but heats to supercritical temperatures during mixing and combustion. The term "transcritical" has often been used to describe this process.

Many fundamental questions remain to be answered regarding the physical behavior of the propellant jets and other phenomena governing the combustion instability. One such question is how the fuel and oxidizer jets change behavior during an unstable combustion event. One early study by Heidmann [3] investigated the behavior of liquid oxygen (LOX) jets in a coaxial-jet-like injector during a period when combustion instability was induced. The LOX jet became shorter once the combustor became unstable. Similar observations were made by Miesse [4] and Buffum and Williams [5] under cold flow conditions when a single round jet was excited with an externally-forced acoustic field.

Mixing of the propellant streams, if not controlling, is at least intimately related to the combustion process. To a first order approximation, one measure of the mixing process is the so-called liquid-core length, which has been extensively studied by many researchers in the past [6-24]. A compilation of experimental core-length correlations, semi-empirical theories, and other data for shear coaxial injector studies involving core length is summarized in Table 1. Many of the correlations and semi-empirical theories reviewed indicate scaling of the core length with outer-jet to inner-jet velocity ratio (V_r), outer-jet to inner-jet momentum flux ratio (M), density ratio (ρ_o/ρ_i), Reynolds number (Re), and Weber number (We). One difficulty with applying these relationships at supercritical pressures is that the predicted core length is very small or zero in magnitude, because one of the parameters in the equation is We and surface tension diminishes greatly or vanishes all together. To overcome the difficulty of core length prediction associated large We, one group of researchers [15-20], proposed that M can be used to describe the scaling

*Presently at GE Global Research,Niskayuna, NY

of the core length for shear-coaxial injectors, and need not include *We* if the *We* is sufficiently high.

Chehroudi and co-workers [22-33] have investigated supercritical jet flows at higher Reynolds numbers and turbulent jets of interest to practical applications in propulsion systems. The single round-jet work by Chehroudi et al. [26-32] was produced from two different injectors made from 50 mm long sharp-edged tubes with the inner jet diameters of 0.254 mm and 0.508 mm, (L/D of 200 and 100, respectively). They injected pure N_2 and O_2 into N_2, He, Ar, and mixtures of CO and N_2 and the arrangement was studied with shadowgraphs and Raman imaging. It was determined that the initial growth rate of a supercritical jet was different from that of a subcritical jet. Furthermore, they quantitatively showed that the initial growth rate of a supercritical jet behaved similar to variable-density gas jets [29]. From this observation, a phenomenological model of the initial growth rate based upon time scale arguments was proposed which agreed well with the results acquired under subcritical and supercritical pressures [29]. It is also important to note that Chehroudi et al. [30] showed that the growth rate measured from shadowgraphs was about twice as large as the growth rate of the jet measured by Raman imaging of the jet, based on the full width at half maximum (FWHM) jet thickness values. The fractal dimension of the initial region of the jet under subcritical and supercritical pressures was also measured by Chehroudi et al. [27, 30, 32] and compared to the fractal dimension of other liquid and gas jets. It was found that the fractal dimension of supercritical jets was similar to that of gas jets, while the fractal dimension of the subcritical jets was similar to that of other liquid jets.

Experimental Setup

The experimental facility, shown in Fig. 1, has been described in detail previously [22-24, 31, 38], so only a brief description will be given here. High-pressure gaseous nitrogen (GN_2) flows into the system and its flow rate is controlled with micrometer needle valves. Temperature conditioning is accomplished by passing the GN_2 through a shell-and-tube type heat exchanger using liquid nitrogen (LN_2) to cool the GN_2. The nitrogen flows into both the inner and outer tubes. The temperature of the flow to the inner round jet of the shear-coaxial injector is considerably lower than that of the outer annular jet, reaching the liquid (subcritical) or densified (supercritical) state. However, the outer jet is cooled well below the room temperature, but is still in gaseous state. The chamber is pressurized with GN_2 at ambient temperature. For reference, the critical pressure and temperature of N_2 is 3.4 MPa and 126.2 K, respectively. The pressure inside the main chamber is maintained by adjusting the outlet flow rate using a triplet of valves to provide an optimum level of control.

The test article consists of a chamber within a chamber. The main, external, chamber is used to create a pressurized environment and is fitted with two sapphire windows for observation of the jet behavior. The smaller, internal chamber, channels and focuses acoustic waves onto the jet at high intensity. The waves are generated by a high pressure acoustic driver developed by Hersch Acoustical Engineering. To obtain sufficiently high amplitudes, the driver must resonate the normal modes of the inner chamber. Therefore, the frequency at which the effects are studied is limited to the first two modes of the inner chamber, being about 3 kHz and 5.25 kHz, respectively. The acoustic wavelength is much longer than the characteristic transverse jet dimensions at both of these frequencies and the conclusions drawn were similar. Consequently, only the 3 kHz results are reported here. The injector is positioned at a pressure node (a velocity anti-node) to produce maximum velocity fluctuations near the jet.

The acoustic driver was always operated at its maximum power, which was the same for all pressures. As a consequence, the acoustic amplitude decreased as pressure increased, due to the increase in density. The amplitude was about 183 dB at 1.49 MPa, about 180 dB at 3.5 MPa, and about 178 dB at 4.9 MPa.

The shear coaxial injector used in this work (see Fig. 2) is based on the well-characterized design of the single-jet injector used in all previous studies [24-30] in this apparatus. The centerpost is made from a stainless steel tube with an I.D. (D_1) of 0.51 mm (0.020") and an O.D. (D_2) of 1.59 mm (0.063") with a length of 50.8 mm (2.00"). This is used to produce the inner jet. The resulting length to inner diameter ratio is 100, which is sufficient to ensure a fully-developed turbulent pipe flow conditions at the exit. The outer stainless steel tube creating the annular passage had an I.D. (D_3) of 2.42 mm (0.095") and an O.D. (D_4) of 3.18 mm (0.125"). This is used to produce the outer coaxial annular jet. The resulting mean gap width of the annular passage is 0.415 mm (0.016"), measured from an image taken at the exit of the injector. The injector has

a small bias of 8% of the mean gap width. The recess of the inner tube was 0.5 D_1, 0.25 mm (0.010") from the end of the outer tube.

Because of the proximity of the experimental conditions to the critical point of nitrogen, accurate measurements of temperature were necessary to obtain reliable estimates of density and other quantities computed from the density. The temperature profiles and the details of the calibration were reported elsewhere (Davis and Chehroudi [22] and Davis et al. [23]).

Shadowgraph images of the jet were taken using either a PixelFly CCD camera or a Phantom v5.1 or v7.1 CMOS camera. The advantage that the CMOS cameras presented was the ability to produce high-speed movies of the jet for a period lasting up to several seconds. The framing rate for the movies in this work was 18 kHz.

Results and Discussion

A. Acoustic Wave Interaction with Shear-Coaxial Jet. High-speed movies of the jet present a large amount of information about the flow being studied. The jets were studied at three different pressures: a subcritical pressure of nominally 1.5 MPa, a near-critical pressure of nominally 3.5 MPa, and a supercritical pressure of nominally 4.9 MPa. A sample of ten consecutive images at the subcritical (rows one and two from top), near-critical (rows three and four), and supercritical (rows five and six) chamber pressures are shown in Fig. 3. Rows one, three, and five are for when the acoustic driver is off and the remaining ones are when it is activated at ~ 3kHz. The evolution of the jet in time is from left to right in Fig. 3, with the time interval between frames of 55.6 μs. Prominent in all the visualizations of the jet is the existence of a dark central region which we refer to as a "dark core". The dark core under the unexcited (i.e. acoustic driver off) subcritical pressures (Fig. 3, row one) can be approximated as a cylindrical-like structure with unstable surface waves of low amplitude. However, upon increasing the pressure to near-critical and supercritical pressures (rows three and five) this structure changes to a more conical shape. The conical structure of the dark core has been reported before for single-phase coaxial jets by Lasheras and Hopfinger [20]. As demonstrated in images of Fig. 3 and the other visualizations obtained in this work (not shown here), the conical-shape structure was not observed under two-phase conditions (i.e., subcritical chamber pressure).

Excitation of the jet with acoustic driver yields significantly different behavior of the dark core compared to that of the unexcited one. The strongest effect was observed at subcritical pressures. It is not clear at this point whether this was due to the subcritical nature of the flow or to the fact that the acoustic amplitude was the highest at subcritical pressures.

It appears from the movies, similar to those used to generate Fig. 3, that as a portion of fluid originating from the inner jet leaves the injector tip, the momentum from the acoustically-induced motion causes a transverse displacement, pushing the core of the jet into the higher speed annular jet. The dense fluid from the core is then accelerated by the outer jet. Upon reversal of the acoustic field, the dense fluid, initially from the core but now in the high-speed annular jet, appears to maintain its transverse component of the momentum imparted upon leaving the injector tip and hence the dense fluid particle does not reverse its direction. The dense fluid parcel then slows (both in the axial and transverse directions) as it arrives at the shear layer between the outer jet and the chamber fluid farther downstream, where a "cusp-shaped" structure is formed from the dense fluid originating in the core of the jet. Subsequent mixing and heat transfer from the outer jet to the inner jet core fluid ultimately causes the fluid parcel to be indistinguishable from the outer jet fluid.

An investigation was also conducted to determine whether the side-to-side oscillation of the jet was occurring in a 3D helical mode or in a 2D planar mode. Visualization of the jet from a direction orthogonal to the perspective of Fig. 3 revealed that the jet oscillation was largely 2D in the direction of the planar acoustic waves.

B. Dark Core Length Measurement Technique. The algorithm for measuring the dark-core length in this work starts with an individual image from which an image histogram is computed. A threshold value is then carefully defined to identify the shape of the dark core of the jet.

It should be mentioned that confusion exists in the literature especially when vague definitions are used to define a core length. The terms potential-core, potential-cone, intact-length, intact-liquid-length, and breakup-length have all been used along with various measurement techniques. To be clear, and to remove any possible ambiguity from the data, the dark-core length is defined here as the connected dark fluid region between the injector exit area and the first break in the core as defined by an adaptive thresholding procedure. See Davis [38] or Davis and Chehroudi [25] for more details.

C. Influence of Velocity Ratio on Dark Core Length. Velocity ratio V_r has been a design parameter for shear-coaxial injectors, particularly, as a criterion to ensure the stable operation of LREs. For LOX/H_2 engines, the design rule-of-thumb has been to keep the velocity ratio greater than about 10 to keep the engine stable, as is discussed by Hulka and Hutt [35]. Although this criterion has been suggested by the experimental data, no physical explanation has been provided. Related to this is a method to rate a LRE for combustion instability, known as temperature ramping. Temperature ramping is accomplished by lowering the temperature of the H_2 while maintaining mass flow rate at a constant value. The lower the H_2 temperature is at the onset of the measured combustion instability, the greater the stability margin that particular LRE is considered to have. Temperature ramping is related to the velocity ratio because one of the effects of lowering H_2 temperature at constant mass flow rate is increased density and consequently lower velocity.

To determine the effects of the outer-jet temperature (which is GN_2 in this work) on the coaxial jet, two nominal temperatures of ~190 K and ~140 K were studied, called "high" and "low," respectively. The averaged dark-core lengths are shown in Figs. 4(a) and 5(a) as a function of velocity ratio (V_r). The RMS of the variations of the dark-core length is also shown in Figs. 4(b) and 5(b). Figures 4 and 5 present results for conditions when the external acoustic field is turned on and off for both nominal high and low outer-jet temperatures. According to Eroglu et al. [10], the average of the length measured from individual images of a set can be regarded as the time averaged value. It should be noted that, for each operating condition in this work, length measurements were also made from an averaged image of a set. In general, the length measured from the averaged image is slightly shorter than the average of the individual dark-core values calculated in a given set.

Evident in Figs. 4(a) and 5(a) is the fact that the length of the dark core decreases as the chamber pressure is increased. The dark core provides an indication of high-density regions of the flow. At a constant chamber pressure, as V_r is increased, the length of the dark core decreases and appears to approach a constant value. In a mean sense, when the dark core feels the imposed external acoustic field, its length is shorter than or equal to that when the acoustic driver is turned off. At the near-critical and supercritical chamber pressures, as the V_r increases, the difference between the lengths of the dark core, measured with and without the acoustic field, diminishes. The RMS values of the dark-core length fluctuations, shown in Figs. 4 (b) and 5(b), exhibit somewhat similar trends to those seen with the mean values. It is known that for a liquid-fueled rocket, atomization and breakup processes, interactions between the propellant jets, droplet formation, and vaporization are all affected by the pressure and, particularly, velocity fluctuations. Also, for any chemically-reacting system, the rate at which energy is released is sensitive to the rate of change of temperature, density, pressure, and, of course, mixture ratio. It is then quite intuitive to relate, in some form, the RMS values of the dark-core length fluctuations to mixture ratio variations. On the other hand, a low RMS value can be interpreted as the jet's inherent steadiness (or insensitivity to external stimuli) and vice versa. Examination of Figs. 4b and 5b clearly shows that this property is drastically reduced as the velocity ratio is increased. It is then quite possible that the observed improvement in combustion stability at higher values of velocity ratio is a result of the inability of the jet to generate large mass flow rate fluctuations under these conditions, weakening a key feedback mechanism for the self-excitation process. In temperature ramping exercises for stability rating of LOX/H_2 engines, the mass flow rate is usually maintained at a constant value [24]. Therefore, as the temperature of the H_2 is decreased during a ramping episode, the H_2 becomes more dense, which decreases the injector velocity ratio. The RMS plots shown here suggest that such a decline in this ratio amplifies the jet's inherent unsteadiness, providing a possible explanation for the engine's eventual arrival into an unstable zone as a temperature ramping test proceeds.

D. Scaling of the Dark Core Length. As mentioned above, the core length has in the past been scaled with many parameters. In some works, *We* and *Re* numbers were used to represent velocity values in nondimensionalized forms, since physical parameters, such as surface tension and viscosity, were not varied. In other works, based on single-phase results, velocity ratio (V_r) or momentum flux ratio (M) were considered to be the scaling parameters. The semi-empirical theory of Rehab et al. [17] produces an equation suggesting that the length of the core scales with $M^{-0.5}$. This equation was then quantitatively compared to single-phase shear-coaxial jet data, often with equal densities [16-18]. Note that for (inner and outer) jets of equal densities,

$M^{-0.5}$ reduces to V_r. The same dependence on M was also reported qualitatively for single-phase shear-coaxial jets of different densities by Favre-Marinet and Samano-Shettini [21]. Additionally, Lasheras et al. [19] stated the applicability of the same $M^{-0.5}$ dependence for two-phase shear-coaxial jets. However, they were unable to make core length measurements from their images.

A plot of the measured dark-core length values, of this work, versus momentum flux ratio is shown in Fig. 6. A clear distinction between the subcritical dark-core length (diamond symbols) and that for the near-critical and supercritical chamber pressures are seen. Subcritical data indicates a much longer length than at supercritical pressures for a given momentum flux ratio. It should be noted that the near-critical pressure data is slightly supercritical, and both the near-critical and supercritical pressure conditions produce a single-phase coaxial jet. The dashed line in Fig. 6 is a least-square curve fit to the subcritical data, and the dotted line is a least squares curve fit to the near-critical and supercritical data. As indicated by the equations on Fig. 6, the single-phase (i.e., near-critical and supercritical pressures) data have the same $M^{-0.5}$ dependence form as reported by others [16-18, 21]. However, the two-phase subcritical data has a weaker dependence, $M^{-0.2}$, than the single-phase dark-core length. Other quantitative differences between the subcritical and supercritical cases have been reported before. For single round jets, Chehroudi and co-workers [29, 30, 32] found that at supercritical pressures the spreading rate and fractal dimension values were the same as those for a gaseous jet injected into a gaseous ambient with different densities (i.e., variable-density, single-phase, gaseous jet). This is similar to the present dark-core length observations. Under supercritical pressures, our coaxial jet scales with $M^{-0.5}$. Therefore, it appears that this form of the dependency on M is not only valid for gas-gas shear-coaxial jets, but for any single-phase shear-coaxial jet.

Figure 7 was constructed with the objective of comparing the dark-core length with all of the available data that exists in the literature for the potential-core length, intact-core length, and breakup-length. This figure represents all of the available data in the literature concerning core length spanning 5 orders of magnitude in momentum flux ratio. Also, note that as M approaches zero, one reaches a limit defining a single round jet configuration because the outer velocity becomes zero. From data in Fig 7, it seems that for $M < 1$, data points converge and approach the core length range expected for single round jets reported by Chehroudi et al. [36] and Oschwald et al. [34]. The single-phase data presented in Fig. 7 follows the dependence of $L/D_1 = A\,M^{-0.5}$, where the constant A is between 5 and 12. At $M > 100$, the experiments of Favre-Marinet and Samano-Shettini [21] exhibit a recirculation bubble at the end of the core, and thus the core length decreases. The injectors used to produce the two-phase coaxial jets of Eroglu et al. [10] and Englebert et al. [12] have much larger outer jet gap widths (see Table 1) than what is typical of rocket injectors. Additionally, the apparatus of Eroglu et al [10], reported in Farago and Chigier [37], does not produce fully-turbulent inner jet until when $Re > 10^4$. The lack of a fully-turbulent inner jet and the significant differences between their injector and shear-coaxial ones used in rockets could be the reason why the core length measured by Eroglu et al. [10] is shorter than those observed in our work. Englebert et al. [12] reported that the core length scaled with $M^{-0.3}$. The core length by Woodward [11] for the water potassium iodide solution with helium, however, obeys very nearly the trends for the subcritical data points (i.e., $25M^{-0.2}$). Considering that momentum flux ratios near 10 are of importance for LRE, to the best of the authors' knowledge, the data for the subcritical (two-phase) case is the only reported information in the neighborhood of the $M = 10$.

Summary and Conclusions

A non-reacting flow study of a cryogenic shear-coaxial injector was conducted at pressures spanning subcritical to supercritical values. The flow from the inner jet of the coaxial injector was liquid nitrogen (or liquid-like, if at supercritical pressures) and cold gaseous nitrogen flowed from the outer annular jet, both injected into a chamber pressurized with nitrogen at room temperature. The resulting coaxial jet was imaged with a camera framing at a rate of up to 18 kHz. The jet was excited transversely with a high-amplitude acoustic driver, with the jet located at a pressure amplitude minimum. The following conclusions are offered:

1. The existence of high-amplitude acoustic waves alters the behavior of the shear-coaxial jet. The resulting structure of the jet exhibits a periodic shape corresponding to the transverse-velocity field created by the acoustic waves. The periodic oscillations imposed on the dark core of the jet is predominately in the direction of the transverse acoustic velocity. No helical mode for the jet was observed.

2. The root mean square (RMS) variation of the dark-core length decreases with increasing velocity ratio at a given chamber pressure and asymptotically approaches a constant level. The RMS of the dark-core length is greatest at subcritical pressures.

3. Previous research showed that an episode of so-called "temperature ramping", used for stability rating, could lead the engine to an unstable behavior. Also, from other research, it is shown that coaxial injectors with high outer-to-inner jet velocity ratios (greater than ~10 for LOX/H2) tend to be more stable. In the current work, the observation that the RMS of the dark-core length fluctuations decreased at high velocity ratio under both high and low outer-jet temperatures is considered to be a potential explanation observed combustion instability behavior. It is possible that decreases in the RMS fluctuation levels could weaken a key feedback mechanism for the self-excitation process that could be driving combustion instability in rocket engines. This offers a possible improvement in understanding of the combustion instability in LRE. Ultimately, this hypothesis requires further testing in a multi-element, fired rocket experimental facility.

4. The quantitative behavior of the dark-core length of the coaxial jet at near- and supercritical pressures follows a similar momentum flux ratio (M) dependency reported for the single-phase shear-coaxial jets (i.e., $12M^{-0.5}$). The dark-core length for the subcritical chamber pressures, however, scales with $M^{-0.2}$.

5. Within a range of momentum flux ratios in between 1 and 10, the dark-core lengths for the coaxial jet under the subcritical (two-phase) ambient pressure used here appear longer than those measured at the supercritical (single-phase) condition. This range represents relevant values for liquid rocket engines, subcritical data define a new regime which was not reported previously.

Acknowledgments

The authors would like to recognize Mr. Mike Griggs for his valuable contributions in the improvements to the experimental facility. Lt. Matthew Raskie, Lt. Jason Szuminski, Mr. Earl Thomas, Mr. Randy Harvey, Mr. David Hill, and Mr. Mark Wilson are thanked for their efforts. Additionally, Ms. Jennie Paton is thanked for making literature available in a timely manner. A great appreciation is extended to Mr. Steven Martin for loaning the authors one of the Phantom Cameras. A special gratitude is expressed to M. Favre-Marinet, E. B. Camano Schettini, and R. D. Woodward for providing us with their core length data in tabular form. D. W. Davis would like to thank his thesis advisor, Dr. R. J. Santoro, for many helpful discussions and permitting his thesis work to be performed off-campus at AFRL. This work is sponsored by the Air Force Office of Scientific Research under Dr. Mitat Birkan, program manager.

References

1. Harrje, D. T. and Reardon, F. H. (eds.), *Liquid Propellant Rocket Combustion Instability*, NASA SP-194, 1972.
2. Yang, V. and Anderson, W. (eds.), *Liquid Rocket Engine Combustion Instability*, Progress in Astronautics and Aeronautics, AIAA, Washington, DC, 1995.
3. Heidmann, M. F. *Oxygen Jet Behavior During Combustion Instability in a Two-Dimensional Combustor*, NASA TN D-2725, 1965.
4. Miesse, C. C., *Jet Propulsion*, Vol. 25, 1955, pp. 525-530, 534.
5. Buffum, F. G., and Williams, F. A., *Proceedings of the 1967 Heat Transfer and Fluid Mechanics Institute*, Edited by P. A. Libby, D. B. Olfe, and C. W. Van Atta, 1967, pp. 247-276.
6. Forstall, W., and Shapiro, A. H., *J. Applied Mechanics*, Trans. ASME, Vol. 72, 1950, pp. 399-408.
7. Chigier, N. A., and Beer, J. M., "The Flow Region Near the Nozzle in Double Concentric Jets," *J. of Basic Engineering*, Trans. ASME, Vol. 4, 1964, pp. 797-804.
8. Champagne, F. H., and Wygnanski, I. J., *International Journal of Heat and Mass Transfer*, Vol. 14, 1971, pp. 1445-1464.
9. Au, H., and Ko, N. W. M., *Journal of Sound and Vibration*, Vol.116, No. 3, 1987, pp. 427-443.
10. Eroglu, H., Chigier, N., and Farago, Z., *Physics of Fluids A*, Vol. 3, No. 2, Jan. 1991, pp. 303-308.
11. Woodward, R. D., "Primary Atomization of Liquid Jets Issuing from Rocket Engine Coaxial Injectors," Ph.D. Dissertation, Department of Mechanical Engineering, The Pennsylvania State University, University Park, PA, 1993.
12. Englebert, C., Hardalupas, Y., and Whitlaw, J. H., *Proc. R. Soc*., Vol. 451, London, 1995, pp. 189-229.
13. Carreau, J. L, Porcheron, E.., LeVisage, D., Prevost, L., and Roger, F., *Int. J. of Fluid Mech. Research*, Vol. 24, Nos. 4-6, 1997, pp.498-507.
14. Porcheron, E.., Carreau, J. L., Prevost, L., LeVisage, D., and Roger, F., *Atomization and Sprays*, Vol. 12, 2002, pp. 209-227.
15. Villermaux, E., Rehab, H., and Hopfinger, E. J., *Meccanica*, Vol. 29, 1994, pp. 393-401.
16. Rehab, H., Villermaux, E., and Hopfinger, E. J., *AIAA Journal*, Vol. 36, No. 5, 1998, pp. 867-869.
17. Rehab, H., Villermaux, E., and Hopfinger, E. J., *J. Fluid Mech*., 1997, pp.357-381.

18. Villermaux, E., *J. Propulsion and Power*, Vol. 14, No. 5, 1998, pp. 807-817.
19. Lasheras, J. C, Villermaux, E., and Hopfinger, E. J., *J. Fluid Mech.*, Vol. 357, 1998, pp. 351-379.
20. Lasheras, J. C., and Hopfinger, E. J., *Annual Rev. Fluid Mech.*,Vol. 32, 2000, pp. 275-308.
21. Favre-Marinet, M., and Camano Schettini, E. B., *International Journal of Heat and Mass Transfer*, Vol. 44, 2001, pp. 1913-1924.
22. Davis, D. W. and Chehroudi, B., *42nd AIAA Aerospace Sciences Meeting & Exhibit*, AIAA, Washington, DC, 5-8 Jan. 2004.
23. Davis, D. W., Chehroudi, B., and Sorensen, I. Measurements of an Acoustically Driven Coaxial Jet under Supercritical Conditions *43rd AIAA Aerospace Sciences Meeting & Exhibit*, AIAA, Washington, DC, 10-13 Jan. 2005.
24. Davis, D. W., and Chehroudi, B.,Measurements of an Acoustically Driven Coaxial Jet under Sub-, Near-, and Supercritical Conditions *J. of Propulsion and Power*, 2005 (submitted).
25. Davis, D. W., and Chehroudi, B., 2006. Shear-Coaxial Jets from a Rocket-Like Injector in a Transverse Acoustic Field at High Pressures. 44ed AIAA Aerospace Sciences Meeting and Exhibit, Paper No. AIAA-2006-0758, Reno, Nevada, January 9-12.
26. Chehroudi, B., Talley, D., and Coy, E. B., *37th AIAA Aerospace Science Meeting and Exhibit*, AIAA, Washington, DC, 11-14 Jan. 1999.
27. Chehroudi, B., Talley, D. G., and Coy, E. B., "Fractal Geometry and Growth Rate Changes of Cryogenic Jets near the Critical Point," *35th AIAA/ASME/SAE/ASEE Joint Propulsion Conference and Exhibit*, AIAA, Washington, DC, 20-24 Jun. 1999.
28. Chehroudi, B., Cohn, R., Talley, D. G, and Badakhsan, A., "Raman Scattering Measurements in the Initial Region of Sub- and Supercritical Jets," *36th AIAA/ASME/SAE/ASEE Joint Propulsion Conference and Exhibit*, AIAA, Washington, DC, 17-19 Jul. 2000.
29. Chehroudi, B., Talley, D. G., and Coy, E. B. "Visual Characteristics and Initial Growth Rates of Round Cryogenic Jets at Subcritical and Supercritical Pressures," *Physics of Fluids*, Vol.4, No. 2, Feb. 2002. pp. 850-861.
30. Chehroudi, B., Cohn, R., and Talley, D. G., "Cryogenic Shear Layers: Experiments and Initial Growth Rates of Round Cryogenic Jets at Subcritical and Supercritical Pressures," *International Journal of Heat and Fluid Flow*, Vol. 23, 2002, pp. 554-563.
31. Chehroudi, B., and Talley, D. G., "Interaction of Acoustic Waves with a Cryogenic Nitrogen Jet at Sub- and Supercritical Pressures," *40th AIAA Aerospace Meeting and Exhibit*, AIAA, Washington, DC, 14-17 Jan. 2002.
32. Chehroudi, B. and Talley, D., "Fractal Geometry of a Cryogenic Nitrogen Round Jet Injected into Sub- and Super-critical Conditions", *Atomization and Sprays*, Vol. 14, 2004, pp. 81-91.
33. Chehroudi, B., Davis, D. W., and Talley, D. G., "Initial Results from A Cryogenic Coaxial Injector In An Acoustic Field," *41st AIAA Aerospace Sciences Meeting & Exhibit*, AIAA, Washington, DC, 6-9 Jan. 2003.
34. Oschwald, M., Smith, J. J., Branam, R., Hussong, J., Schik, A., Chehroudi, B., and Talley, D. G., "Injection of Fluids into Supercritical Environments," *Comb. Sci. Tech.*, Accepted, 2005.
35. Hulka, J., and Hutt, J., "Liquid Oxygen / Hydrogen Instability Phenomena," Liquid Rocket Engine Combustion Instability, edited by V. Yang and W. Anderson, *Progress in Astronautics and Aeronautics*, AIAA, Washington, DC, 1995, pp. 39-72.
36. Chehroudi, B., Chen, S. H., Bracco, F. V., and Onuma, Y., 1985. On the Intact Core of Full-Cone Sprays, Society of Automotive Engineers, 1985 Congress and Exposition, *SAE Transaction Paper 850126*, February 25-March 1.
37. Faragó, Z., and Chigier, N., "Morphological Classification of Disintegration of Round Liquid Jets in a Coaxial Air Stream," *Atomization and Sprays*, Vol. 2, 1992, pp. 137-153.
38. Davis, D. W., "On the Behavior of a Shear-Coaxial Jet Spanning Sub- to Supercritical Pressures, with and without an Externally Imposed Transverse Acoustic Field", Ph.D. Dissertation, Department of Mechanical Engineering, The Pennsylvania State University, University Park, PA, 2006.

Table 1. Summary of published operating conditions, geometries, measurement techniques, and proposed equations from the literature, measuring or correlating core length for shear-coaxial jets.

REF	Author	Date	Fluid Inner Jet	Fluid Outer Jet	Fluid Ambient	Pressure (MPa)	T_i (K)	T_o (K)	T_∞ (K)
6	Forstall & Shapiro	1950	Air+ 10 %He	Air	Air	0.1*	Amb. [a]	Amb.	Amb.
7	Chigier & Beer	1964	Air	Air	Air	0.1*	Amb.	Amb.	Amb.
8	Champagne & Wygnanski	1971	Air	Air	Air	0.1	Amb.	Amb.	Amb.
9	Au and Ko	1987	Air	Air	Air*	0.1*	Amb.	Amb.	Amb.
10	Eroglu et al.	1991	Water	Air	Air	0.1*	Amb.	Amb.	Amb.
11	Woodward	1993	KI (aq.)	N2, He	N2, He	0.1 – 2.17	Amb.	Amb.	Amb.
15	Villermaux et al.[g]	1994	Water	Water	Water	0.1*	Amb.	Amb.	Amb.
12	Englebert et al.	1995	Water	Air	Air	0.1	293	293 – 636	293
13	Carreau et al.	1997	LOX	He, N2, Ar	NC[c]	0.1	82[d]	245 – 272[d]	NC
16	Rehab et al.[g]	1997	Water	Water	Water	0.1*	Amb.	Amb.	Amb.
17	Rehab et al.[g]	1998	Water	Water	Water	0.1*	Amb.	Amb.	Amb.
18	Villermaux [g,h]	1998	Water	Water	Water	NR	NR	NR	NR
19	Lasheras et al.[g]	1998	Water	Air	Air	0.1	Amb.	Amb.	Amb.
20	Lasheras & Hopfinger [g,i]	2000	NR	NR	NR	NR	NR	NR	NR
21	Favre-Marinet & Schettini	2001	Air, SF6	Air,He	Air, He	0.1	Amb.	Amb.	Amb.
14	Porcheron et al.	2002	LOX, Water	He, N2, Ar, Air	Air	0.1	82, 293	245 – 293	293
This work	Davis	2005	N2	N2	N2	1.4 – 4.9	108 – 133	132 – 204	197 – 249

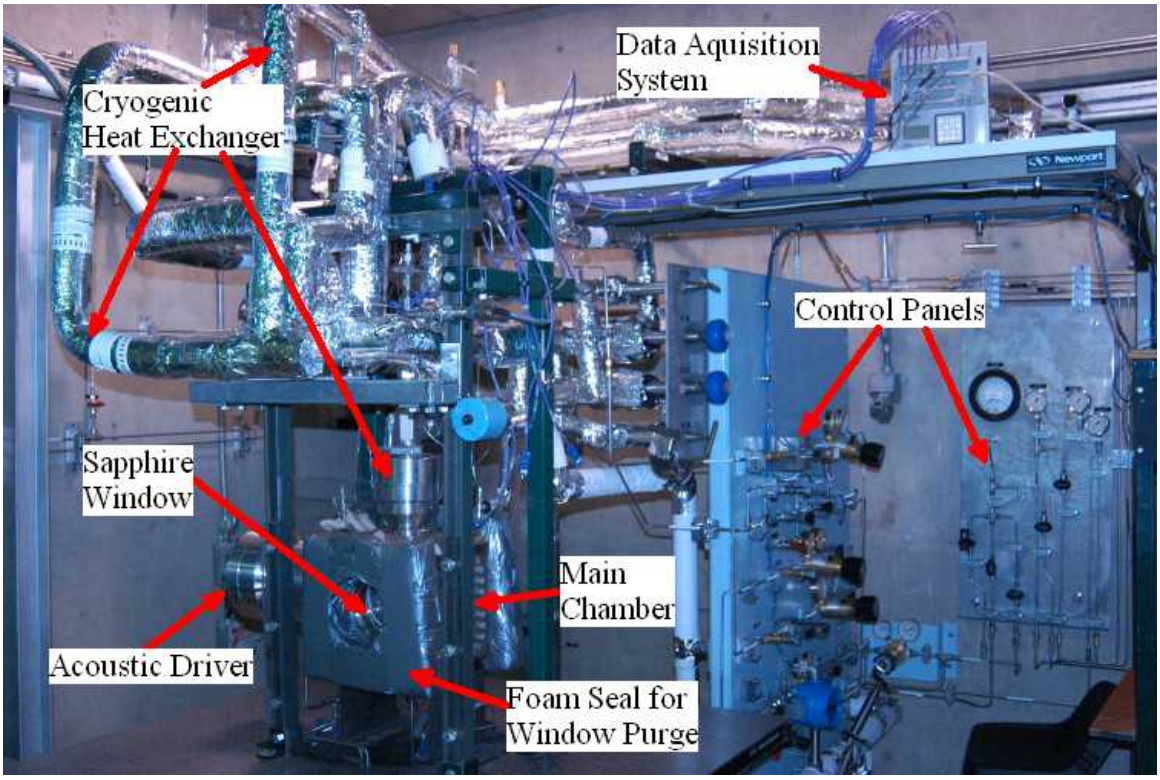

Figure 1. Picture of the experimental facility

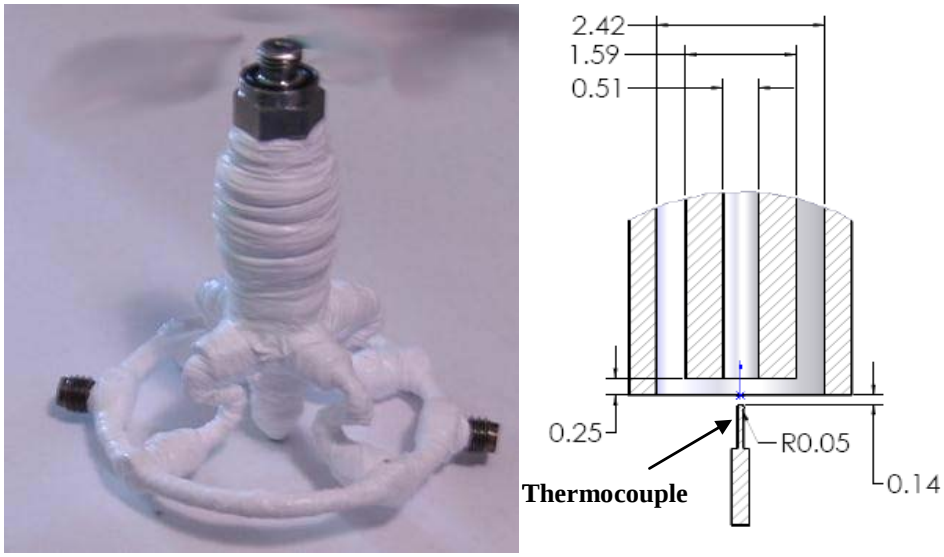

Figure 2. Picture of the shear-coaxial injector (left) and a cross-section drawing of the injector tip. The thermocouple used to measure exit-plane temperature profiles is shown in the drawing.

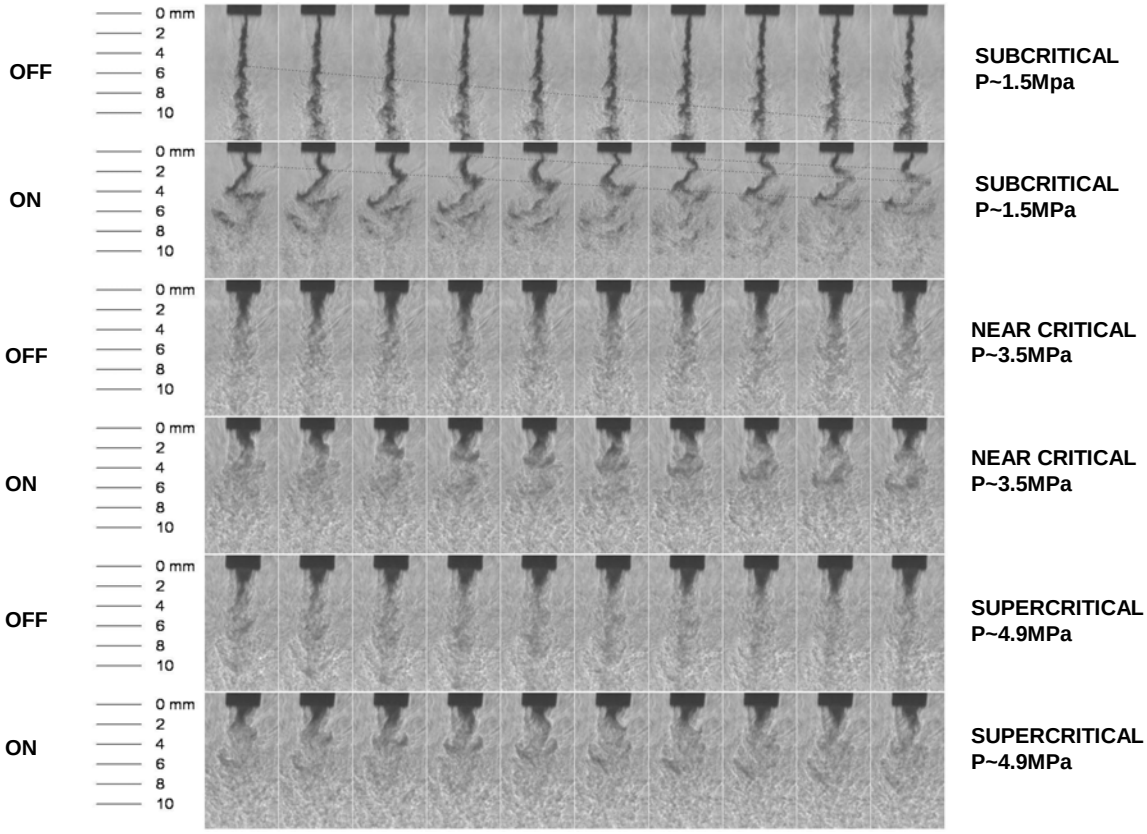

Figure 3. Consecutive frames from high-speed shadowgraph movies with the acoustic driver turned off (in rows 1, 3, and 5) and on (in rows 2, 4, and 6) at ~3kHz. Time increases from left to right with an interval of 55.6 ms between frames. The first two rows are at a subcritical chamber pressure (~ 1.5 MPa), the third and fourth rows are at a near-critical chamber pressure (~ 3.5 MPa), and the fifth and sixth rows are at a super-critical chamber pressure (~ 4.9 MPa). The acoustic driver is turned off for the first, third, and fifth rows and on for the second, fourth, and sixth at ~ 3 kHz. The light gray lines in the first and second rows connect fluid structure as they evolve in time.

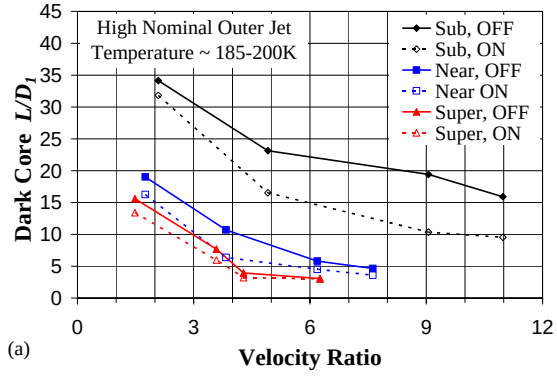

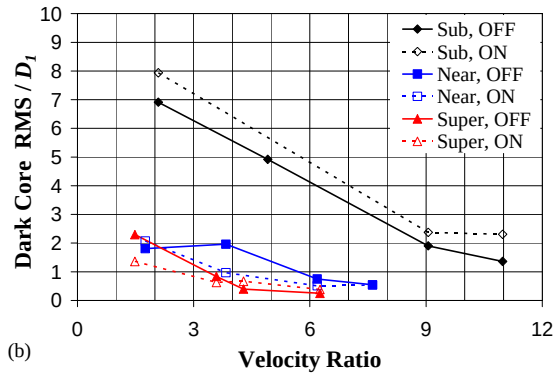

Figure 4. Plot of the averaged dark-core length (a) and the RMS of the length variations (b) normalized by the inner diameter. The solid symbols and lines represent the data for when the acoustic driver is off, and the hollow symbols and dotted lines show the data when the acoustic driver was operated at ~ 3kHz. The diamond, square, and up-triangle symbols are sub-, near, and supercritical chamber pressures, respectively. All cases are for the high nominal outer-jet temperature of ~190 K. In the inset, the words sub, near, and super refer to subcritical, nearcritical, and supercritical pressure respectively, and the words OFF and ON refer to the acoustic driver being off and on at ~3kHz, respectively.

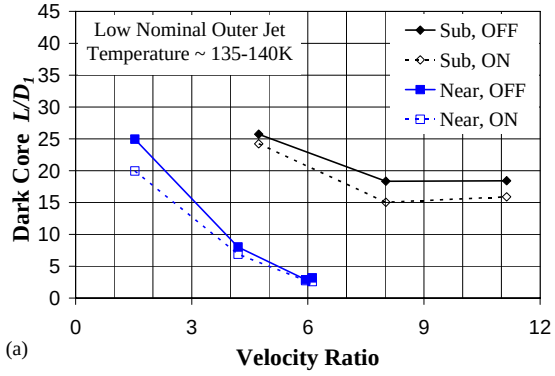

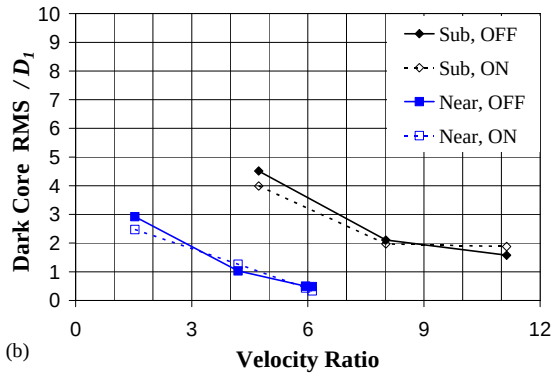

Figure 5. Plot of the averaged dark-core length (a) and the RMS of the length variations (b) normalized by the inner diameter. The solid symbols and lines represent data for when the acoustic driver is off, and the hollow symbols and dotted lines show results when the acoustic driver is operated at ~ 3kHz. The diamond and square symbols are for sub- and near-critical chamber pressures, respectively. All cases are for the low nominal outer-jet temperature of ~140 K. In the inset, the words sub and near refer to subcritical and nearcritical pressure respectively, and the words OFF and ON refer to the acoustic driver being off and on at ~3kHz, respectively.

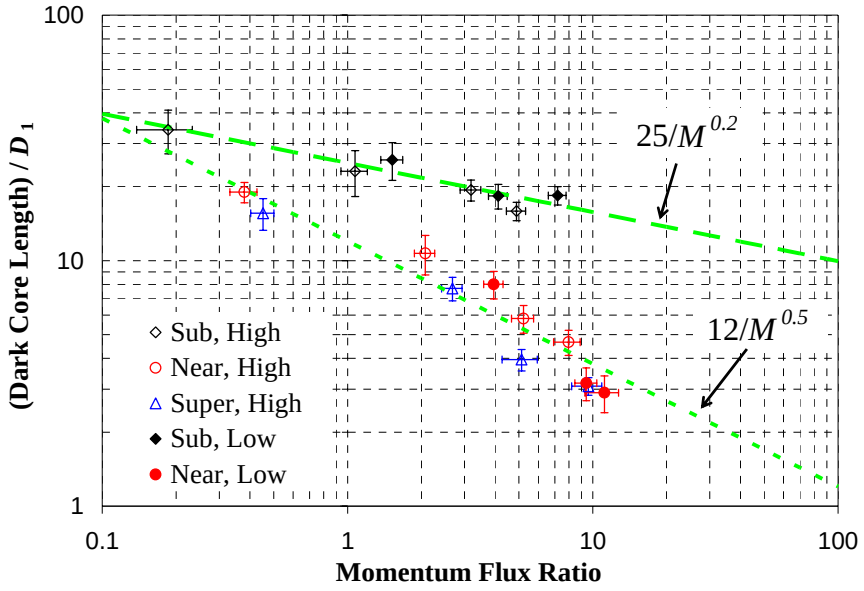

Figure 6. Dark-core length versus momentum flux ratio. The diamond, circle, and up-triangle symbols represent sub-, near-, and supercritical chamber pressure, respectively. The hollow symbols are at a high outer-jet temperature (~190 K) and solid symbols are at a low outer-jet temperature. The dashed line is $25/M^{0.2}$ and the dotted line is $12/M$

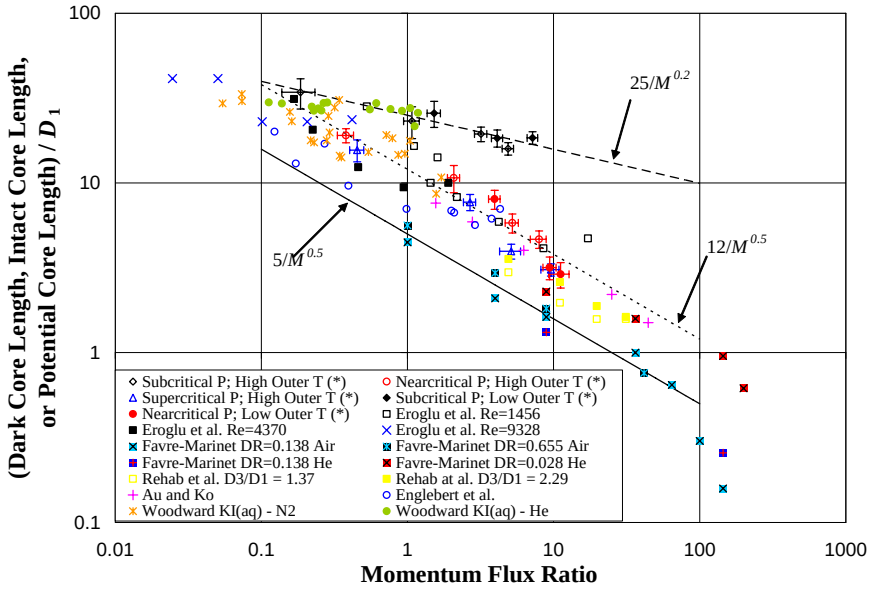

0.5.

Figure 7. Comparison of the present dark-core length measurements with all other core length data available in the literature vs. momentum flux ratio. Amongst the data reported by others, Eroglu et al., Englebert et al. and Woodward are two-phase flows and the rest are single phase.